Turk J Chem
34 (2010) , 465 – 479.

doi:10.3906/kim-0903-4

Electrochemical properties of 1-($o-$, $m-$, p-nitrophenyl)-3-($m-$nitrophenyl)-5-phenylformazans and their nickel complexes

Habibe TEZCAN*, **Mehmet Levent AKSU**
Gazi University, Faculty of Education, Department of Chemistry
Teknikokullar, 06500 Ankara-TURKEY
e-mail: habibe@gazi.edu.tr

Received 02.03.2009

The electrochemical properties of NO_2 formazans and their Ni(II) complexes were investigated. The investigated formazans included a NO_2 group at the $o-$, $m-$, and $p-$ positions of the 1-phenyl ring and at the $m-$ position of the 3-phenyl ring. The oxidation and reduction peak potentials, number of electrons transferred, diffusion coefficient, heterogeneous rate constant, and possible reaction mechanism of the compounds were determined with the use of cyclic voltammetry (CV), ultramicrodisc electrodes (UMEs), and chronoamperometry (CA). The peak potentials ($\mathbf{E}_{ox1}$) were observed to shift towards more anodic potentials in formazans and more cathodic potentials in their respective Ni complexes compared to unsubstituted compounds. There was a correlation between their absorption and electrochemical properties. The electrochemical reaction mechanism was observed to be dependent upon the type and position of the substituent in the structure. Nicholson and Shain criteria showed that the reaction follows an EC mechanism.

Key Words: Formazans, nickel complexes, spectroscopy, substituent effect, cyclic voltammetry, ultramicrodisc electrode.

Introduction

Formazans and their metal complexes are colored compounds due to $\pi - \pi^*$ transitions of π-electrons in the formazan skeleton of -N=N-C=N-NH-. This has caused intensive interest among scientists. Since the synthesis of the first formazans by Pechman there have been numerous formazans prepared and their structural features,

*Corresponding author

and tautomeric and photochromic isomers have been investigated.[1–4] Their derivatives with electron donating and withdrawing groups attached to the 1,3,5-phenyl ring were prepared and the effects of substituents on the absorption $\lambda_{\max}$ values were examined.[5–8]

Metal complexes of formazans are colored compounds. That is why they have been subjected to thorough investigation. It was determined that the formation of Fe complexes was dependent upon the pH value. The structural determination, complex stability constants, and spectroscopic features of metal complexes of formazans were widely investigated.[9–16]

Formazans form tetrazolium salts when they are oxidized.[17] Tetrazolium salts are reduced back to formazans by the enzymes in the cell and stain the tissue. That is why the tetrazolium-formazan system is classified as a marker of vitality.[18] This feature enables the determination of activity of tumor cells, which caused increasing interest in the chemistry and especially in the spectral and the electrochemistry of formazans.[19] It was claimed that tetrazolium salts give 1 electron transfer reduction, resulting in radical formation, which gives either a disproportionation or dimerization reaction forming a diformazan.[20] Formazans were reported to be oxidized in a single step 2 electron transfer followed by a deprotonation reaction forming corresponding tetrazolium cations and the tetrazolium salts.[21,22]

The electrochemical behavior of some substituted formazans has been extensively studied.[23–26]

This study was carried out in 2 stages. The first stage involved the synthesis of 4 different formazans and their nickel(II) complexes with NO_2 on the 1- and 3-phenyl rings (**Scheme 1**). Their structural and spectral properties and the effect of substituents on $\lambda_{\max}$ values have been previously reported.[8,11] The biological activity of formazans makes knowledge of their oxidation potentials and their possible mechanisms very important. That is why the second stage dealt with the investigation of their electrochemical behaviors such as peak potentials (E_{ox}, E_{red}), diffusion coefficients (D), the number of electrons transferred (n), and heterogeneous rate constants (k_s). A mechanistic oxidation scheme for tetrazolium salt was proposed based upon these data. It is hoped that they are suitable for medical, analytical, and drug applications, and the dye industry.

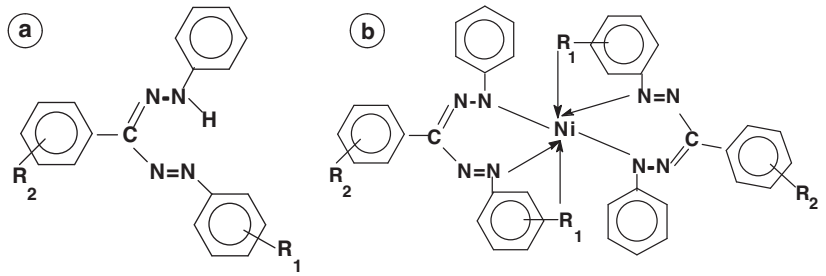

Formazasns (a)	R_1	R_2	Ni-comp. (b)
1a	H	H	**1b**
2a	*o*-NO_2	*m*-NO_2	**2b**
3a	*m*-NO_2	*m*-NO_2	**3b**
4a	*p*-NO_2	*m*-NO_2	**4b**

Scheme 1. Chemical structures of the formazans investigated and their nickel(II) complexes.

Experimental

Chemicals

1,3,5-Triphenylformazan and its NO_2 derivatives 1-($o-$, $m-$, $p-$nitrophenyl)-3-($m-$nitrophenyl)-5-phenylformazans **(1a-4a)** and their nickel complexes (**1b-4b**) were prepared as described in the literature,[8,11] and the compounds were purified by recrystallization until sharp melting points were obtained. The structures of the compounds were elucidated by using elemental analysis, GC-Mass, ^{1}H-NMR, ^{13}C-NMR, IR, and UV-vis spectra and spectral behaviors have been reported.[8,11]

All the other chemicals were purchased from Merck and Sigma-Aldrich. Deionized water (Millipore, Milli-Q), CH_3OH (99.9%), CH_3COCH_3 (99.9%), and dioxane were used for the synthesis and absolute dry dimethylsulfoxide (DMSO) (99.99%) was used for the spectroscopic and the electrochemical measurements. The supporting electrolyte, tetrabutylammonium tetrafluoroborate (TBATFB), was purchased from Fluka (21796-4), used without further purification, and kept in a desiccator.

Measurements

Electrochemical studies were carried out with a computerized CHI Instrument 660 B system in a conventional 3-electrode cell. A platinum electrode (PE) (CHI102) and a 10 μm-platinum ultramicro disc electrode (UME) (CHI107) were used as working electrodes. The real surface area of the Pt electrode was found to be 2.58 cm^2 with the use of ferrocene. The electrodes were cleaned by electrochemical potential cycling and washing with excess DMSO. A platinum wire was used as the auxiliary electrode. The reference electrode was a silver wire in contact with 0.1 M $AgNO_3$ in DMSO. All solutions were deaerated for 10 min with pure argon and blanketed thereafter and the measurements were obtained at 25 °C. Tetrabuthylammonium tetrafluoroborate ($TBA^+BF_4^-$) was purchased from Fluka (21796-4) and used without purification. DMSO was used as a solvent, keeping its ionic strength at 0.1 M, with TBATFB as a supporting electrolyte.

Method

The number of electrons transferred (n) and the diffusion coefficients (D) were determined from the Cottrell equation by the ultramicroelectrode CV technique of Baranski.[27] The heterogeneous rate constants k_s were calculated according to the Klingler-Kochi method.[28]

Results and discussion

This study was carried out to explain the electrochemical behaviors. However, the evaluation of the UV-vis data will be briefly discussed for comparison with the electrochemical results.

Substituent effect on the UV-vis absorption λ_{max} values

Table 1 lists all the peaks observed in the UV-vis spectra of formazans (**2a-4a**) and related nickel(II) complexes (**1b-4b**). The chemical shift values ($\Delta\lambda$) were determined by taking the difference between the λ_{max} value of

1a with $\lambda_{\max}$ values of **2a-4a** and the $\lambda_{\max}$ value of **1b** with $\lambda_{\max}$ values of **2b-4b** (Column 3). As seen in Table 1, the $\lambda_{\max}$ value of **1a** is 482 nm. These values shifted 484, 473, and 478 nm when the 1–phenyl ring is substituted with a NO_2 group at the $o-$, $m-$, and $p-$positions, respectively, while the 3-phenyl ring is substituted with a NO_2 group at the $m-$position (**2a-4a**).

Table 1. UV-visible absorption maxima of the formazans (**1a-4a)** and its nickel(II) complexes (**1b-4b)** (DMSO, 10^{-5} mol/L).

No	λ_{max1}/ nm- (Abs)	Formazan $\Delta\lambda^a_{max}$ nm Ni.comp. shifts $\Delta\lambda^b_{max}$ nm	NiComp.-Formaz. $\Delta\lambda_{max}$nm
1a	482.0 -(0.630)	-	
2a	484.0 -(0.650)	-2	
3a	473.0 -(0.402)	9	
4a	478.0 -(0.610)	4	
1b	611.0 -(0.067)	-	129
2b	607.0 -(0.079)	4	123
3b	613.0 -(0.045)	2	140
4b	617.0 -(0.030)	6	139

Column 3: $\Delta \quad \lambda^a_{\max} = \lambda_{\max 1}$(TPF)- $\lambda_{\max 1}$ (substituted formazans)
Column 3: $\Delta \quad \lambda^b_{\max} = \lambda_{\max 1}$ (Ni-TPF)- $\lambda_{\max 1}$ (substituted nickel(II) complexes)
Column 4: $\Delta \quad \lambda^c_{\max} = \lambda_{\max 1}$ (substituted TPF)- $\lambda_{\max 1}$ (substituted Ni-TPF)

The NO_2 group in m- and p-NO_2 substituted formazans **3a** and **4a** displays the electron withdrawing effect. The shifts in absorption values $\Delta\lambda_{\max}$ of $m-$ and $p-NO_2$ were merely 9 and 4 nm. In the o-position the nitro group seems to induce a very weak electron donating effect in contrast to expectations. This may be explained by the formation of a hydrogen bond between nitro oxygen and the H-atom on the nitrogen atom of the hydrazone group, which diminishes the electron withdrawing effect of the nitro group by resonance **(Scheme 2).** This behavior was encountered in our previous study.[7]

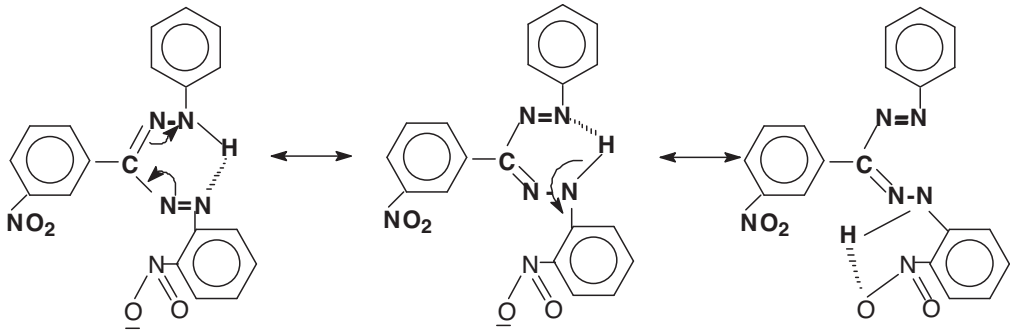

Scheme 2. The formation hydrogen bond between the NO_2 and N-H groups.

$\lambda_{\max}$ values shifted to 617-607 nm in nickel(II) complexes. The magnitudes of the shifts were observed to follow the order of $p- >$ $m- >$ o- substitutions. UV-vis $\lambda_{\max}$ values of formazans were compared against

1a and complexes were compared against **1b** in Figure 1. This can be explained by the formation of a structure with 2 formazan skeletons as a result of the insertion of a Ni^{++} ion, which almost doubled the resonance effect in the complexes. These results are in harmony with the literature.[9,13,15,16]

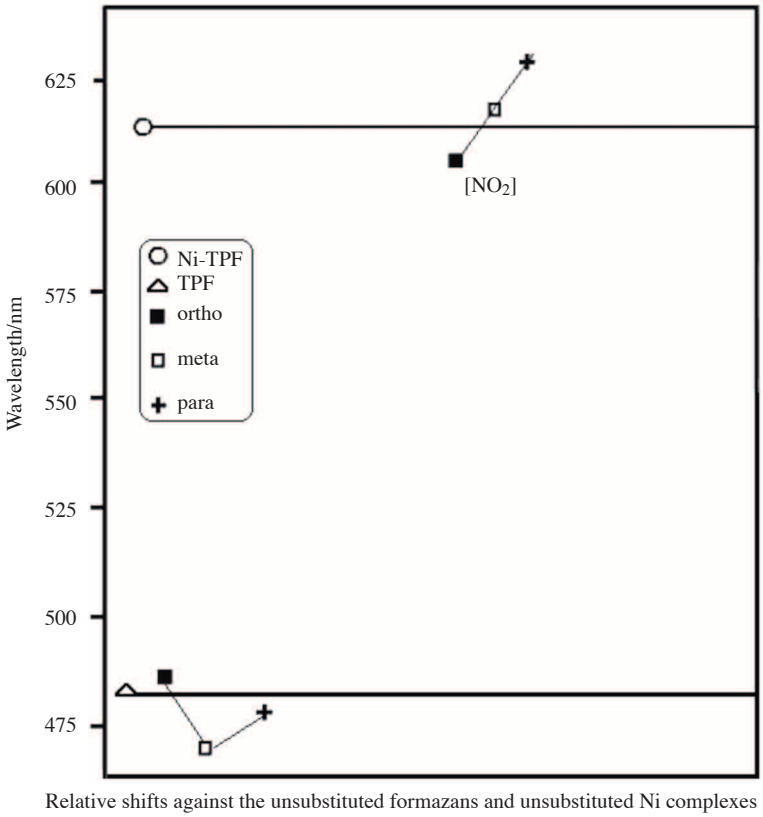

Figure 1. Comparison of the absorption λ_{max} values of **2a-4a** against **1a** and its substituted nickel(II) complexes **2b-4b** against **1b**.

Cyclic voltammetry

The cyclic voltammetric behavior of formazans **1a-4a** and their nickel(II) complexes **1b-4b** were studied in DMSO, at 25 °C and 1.10^{-4} M concentration. The voltammograms were taken over potential range (-2)-(0) V; however, the range used in the study was -1.60 to +0.00 V in the positive potential direction in the forward scan. No peak was observed below or above these potentials. The scan rates employed were 10, 100, 1000, 10000 mV s^{-1} as required in the Nicholson–Shain criteria.

Cyclic voltammogram of Formazans (1a-4a)

All the voltammetry values are shown in Tables 2-4. As seen from Table 2 and Figure 2, the substitution of the 3-phenyl ring with NO_2 at the *m*−positions and 1-phenyl ring with NO_2 at the *o*−, *m*−, and *p*−positions **2a-4a** and **2b-4b** caused changes in both the anodic and cathodic peak potentials and peak currents as compared to **1a** and **1b.**

Table 2. Voltammetry results of formazans (**1a-4a**) and nickel(II) complexes (**1b-4b**).

No	E_{ox1} (mV)	I_{pox1} (A)	E_{ox2} (mV)	I_{pox2} (A)	E_{red1} (mV)	I_{pred1} (A)	E_{red2} (mV)	I_{pred2} (A)	ΔE_p (mV)	$k_s(cms^{-1})$
1a	-1390.3	3.086×10^{-6}	-688.9	1.789×10^{-6}	-426.0	2.657×10^{-6}	-815.1	6.098×10^{-6}	-565.2	7.722×10^{-3}
2a	-1217.4	6.128×10^{-6}	-661.5	1.238×10^{-5}	-581.5	1.900×10^{-5}	-1048.1	3.225×10^{-5}	-635.9	28.078×10^{-3}
3a	-1215.2	4.336×10^{-6}	-675.4	2.501×10^{-6}	-610.0	2.894×10^{-5}	-981.0	6.200×10^{-5}	-605.2	38.215×10^{-3}
4a	-1272.3	3.307×10^{-7}	-785.1	3.499×10^{-6}	-563.0	2.533×10^{-5}	-1037.0	5.917×10^{-5}	-709.3	25.150×10^{-3}
1b	-1260.6	3.086×10^{-6}	-	-	-798.1	2.657×10^{-6}	-	-	-462.5	11.964×10^{-3}
2b	-1544.6	7.337×10^{-6}	-	-	-856.6	1.092×10^{-5}	-1086.0	1.317×10^{-5}	-688.0	41.916×10^{-3}
3b	-1430.6	6.450×10^{-6}	-732.6	2.034×10^{-5}	-808.3	1.402×10^{-5}	-	-	-622.3	37.840×10^{-3}
4b	-1594.8	9.752×10^{-6}	-1068.2	1.338×10^{-5}	-759.4	1.262×10^{-5}	-	-	-835.4	6.908×10^{-3}

Column 10: ΔE_p: E_{ox1}-E_{red1} (mV). Cyclic voltammograms were obtained in DMSO at 25 °C at platinum electrode, ionic strength 0.1 M (TBA $^{+}BF_4^{-}$), sweep speed: 100 mVs^{-1}.

E_{ox}: oxidation; E_{red}: reduction, k_s/cm s^{-1} values.

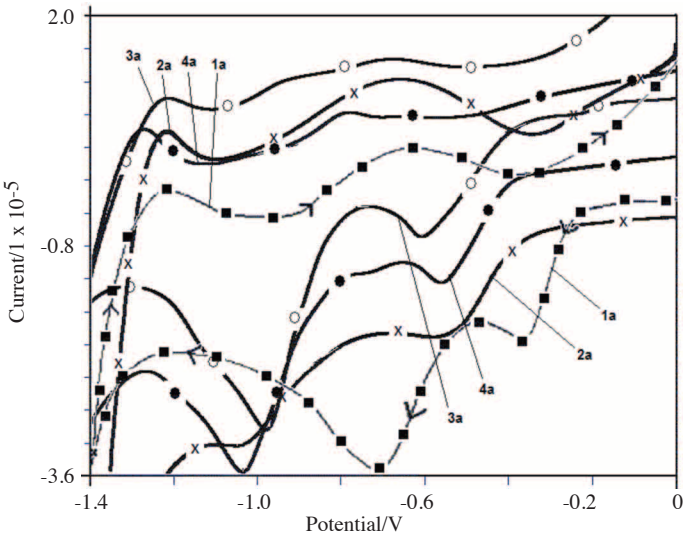

Figure 2. Representative cyclic voltammogram of **1a-4a** (in DMSO, 25 °C, ionic strength: 0.1 M $TBA^+BF_4^-$, ν: 100 mV s^{-1}).

The cyclic voltammograms of **1a-4a** showed 2 anodic waves and 2 cathodic waves. The first anodic peak (E_{ox1}) for **1a-4a** observed at -1390.3 mV, -1217.4 mV, -1215.2 mV, and -1272.3 mV corresponded to the formation of formazan radical (TPF) and the second oxidation peak (E_{ox2}) observed at -688.9 mV, -661.5 mV, -675.4 mV, and -785.1 mV corresponded to the formation of tetrazolium cation (TPT^+). From these results the following stepwise reactions for electron transfer can be given.[22]

$TPF \rightarrow TPF + e^- + H^+$ (electrode, then chemical reactions)

$TPF \rightarrow TPT^+ + e^-$

The oxidation peaks of **2a-4a** shifted to less negative potentials compared to **1a.** This shows that the substitution of NO_2 facilitated the oxidation process. This is quite contrary to the expectations due to the electron withdrawing effect of the nitro group. This may be attributed to the dominance of the mesomeric effect over the electron withdrawing effect. This fact is supported by I_p and k_s values. As seen from Table 2 the reduction potentials of **1a** E_{red1} and E_{red2} were shifted to more cathodic values in **2a-4a**.

These values also showed that the reduction process was also facilitated by the substitution of the NO_2. This is very important for vitality marker features.[18,19] Since marker of vitality features of the triphenyl tetrazolium salts depend on their reduction process, it may be that NO_2 substituted tetrazolium salts to corresponding formazans are more suitable for using as markers of vitality than unsubstituted formazan.

The oxidation of TPF and its nitro derivatives appears to be quasi-reversible, because ΔE_p (E_p^a - E_p^c) are larger than 59/n mV (Table 2). Moreover, as the scan rate increases, anodic peaks become more anodic, cathodic peak potentials become more negative (Table 3), and ΔE_p increases. These results are consistent with quasi-reversible behavior.[30]

As seen from Table 4 the intensity of the first peak for **2a-4a** is higher compared to **1a.** This shows that the electron transfer rate is much higher in NO_2 substituted formazans than in unsubstituted formazans. It seems that the substitution of the NO_2 group has quite an effect upon the electrochemical behavior of formazans.

Table 3. Voltammetric data of formazans (**1a-4a**) and nickel(II) complexes (**1b-4b**) scan rates (in DMSO at platinum electrode and 25 ^{0}C, ionic strength 0.1 M ($TBA^+BF_4^-$), scan rates: 10, 1000 and 10000 mVs^{-1}).

No	Scan rate (mV/s)	E_{ox1} (mV)	I_{pox1} (A)	E_{ox2} (mV)	I_{pox2} (A)	E_{red1} (mV)	I_{pred1} (A)	E_{red2}) (mV)	I_{pred2} (A)
1a	10	-1467.9	2.133×10^{-7}	-	-	-1047.0	2.625×10^{-5}	-	-
	1000	-1311.4	1.111×10^{-4}	-	-	-237.4	3.261×10^{-5}	-	-
	10000	-1298.0	7.896×10^{-6}	-	-	-	-	-	-
2a	10	-1231.4	6.282×10^{-6}	-757.7	3.046×10^{-6}	-540.4	1.057×10^{-5}	-897.1	1.075×10^{-5}
	1000	-1003.7	1.242×10^{-4}	-	-	-1158.4	9.574×10^{-5}	-	-
	10000	-529.1	4.525×10^{-4}	-	-	-1076.5	2.550×10^{-4}	-	-
3a	10	-1242.6	4.481×10^{-6}	-844.7	4.481×10^{-6}	-618.1	1.005×10^{-5}	-938.4	2.197×10^{-5}
	1000	-1051.7	1.628×10^{-4}	-	-	-1066.0	5.675×10^{-5}	-	-
	10000	-624.4	6.972×10^{-4}	-	-	-288.9	6.518×10^{-4}	-	-
4a	10	-1283.7	2.512×10^{-6}	-702.8	2.623×10^{-6}	-997.9	1.612×10^{-5}	-1190.0	2.158×10^{-5}
	1000	-1044.7	1.613×10^{-4}	-	-	-1094.2	4.757×10^{-5}	-	-
	10000	-617.4	6.208×10^{-4}	-	-	-377.2	7.660×10^{-4}	-	-
1b	10	-1477.0	3.923×10^{-6}	-	-	-803.5	5.287×10^{-6}	-	-
	1000	-1168.3	3.430×10^{-6}	-	-	-900.5	2.311×10^{-5}	-	-
	10000	-1632.0	9.499×10^{-6}	-	-	-1144.5	4.219×10^{-5}	-	-
2b	10	-1579.4	4.400×10^{-6}	-	-	-730.1	6.667×10^{-6}	-1044.7	6.858×10^{-6}
	1000	-1437.6	6.293×10^{-7}	-	-	-762.0	1.523×10^{-4}	-	-
	10000	-1106.1	1.795×10^{-5}	-	-	-935.2	1.561×10^{-4}	-	-
3b	10	-1450.9	2.604×10^{-6}	-1051.7	8.747×10^{-7}	-779.9	9.176×10^{-6}	-1221.3	7.729×10^{-6}
	1000	-882.1	2.212×10^{-4}	-	-	-1328.0	2.829×10^{-4}	-	-
	10000	-678.2	2.157×10^{-4}	-	-	-1323.7	2.852×10^{-4}	-	-
4b	10	-1608.5	1.377×10^{-6}	-1215.1	2.747×10^{-6}	-893.3	1.154×10^{-5}	-1330.3	8.973×10^{-6}
	1000	-1449.6	5.804×10^{-5}	-	-	-1052.2	5.684×10^{-5}	-1445.5	6.010×10^{-5}
	10000	-1060.1	1.911×10^{-4}	-	-	-1457.5	2.538×10^{-4}	-	-

Cyclic voltammogram of Ni-Complexes (1b-4b)

Cyclic voltammograms of **1b-4b** are shown in Figure 3. The voltammetric scan showed one anodic wave at E_{ox1} = -1260.6 mV and a cathodic wave at E_{red1} = -798.1 mV for **1b**. **1b** gives one electron transfer. This complex probably gives a dimerization or disproportionation reaction following the radical formation step at -1260.6 mV.[20,25]

The comparison of **1a** and **1b** shows some interesting changes (Figures 2 and 3). The peak related to the formation of the formazan radical completely disappeared and the peak related to the formation of the tetrazolium cation remained almost the same showing a slight anodic shift. This is related to the fact that the insertion of an electron withdrawing nickel(II) cation into the structure decreases the electron density of the system.[24,26]

It seems in Figure 3 that the substituted NO_2 group has quite an effect upon the electrochemical behavior of **2b-4b**. The oxidation behavior of **2b** is the same as that of 1**b**. However, **3b** and **4b** give directly tetrazolium cations (TPT^+) by a single step 2 electron transfer.

Oxidation peaks were observed at more cathodic potentials in **2b-4b** compared with **1b**. The scan of **2b** showed 1 anodic wave and 2 cathodic waves. A cyclic voltammetric sweep shows 1 anodic peak at E_{ox1} =

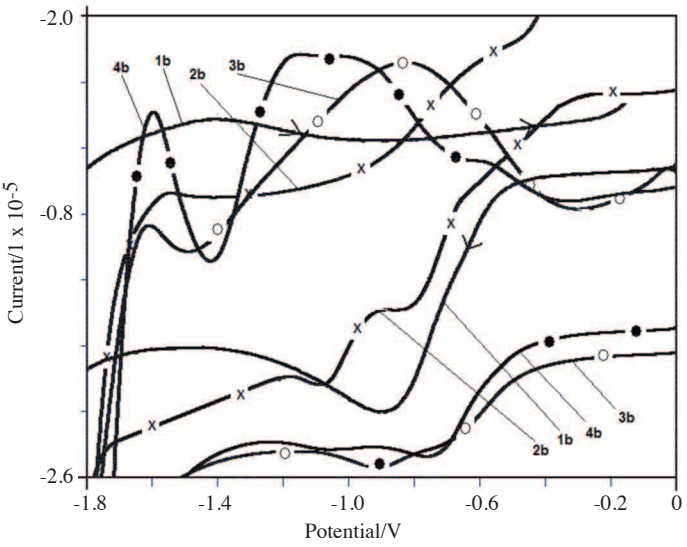

Figure 3. Representative cyclic voltammogram of **1b-4b** (in DMSO 25 °C, ionic strength: 0.1 M $TBA^+BF_4^-$, ν: 100 mV s^{-1}).

-1544.6 mV and 2 cathodic peaks at E_{red1} = -856.6 mV, E_{red2} = -1086.0 mV for **2b.**

When the scan rate was increased, anodic peak potential E_{ox1} was shifted towards anodic values in accordance with a quasi-reversible process. The same situation is valid for **2b-4b.** Table 3 shows the values obtained at different scan rates in order to test the Nicholson and Shain criteria. The plot of current function against $v^{1/2}$ for the first oxidation peak shows that the reaction follows an EC mechanism.[30]

In the -1.60 to +0.00 V range, 2 anodic peaks (E_{ox1}, E_{ox2}) appeared at -1430.6 mV and -732.6 mV, respectively, and 1 cathodic peak (E_{red1}) was observed at -808.3 mV for **3b**. A cyclic sweep shows 2 anodic peaks at E_{ox1} = -1594.8 mV, E_{ox2} = -1068.2 mV and 1 cathodic peak at E_{red1} = -759.4 mV for **4b** (Figure 3). The intensity of the first peak follows the order of $p- > \quad m- > \quad o$-NO_2 substituted nickel(II) complexes. These results are in good accordance with the spectroscopic data. Consequently, peak potentials are dependent upon the type and position of substituents.

Ultramicrodisc electrode and chronoamperometry

The number of electrons transferred (n) and the diffusion coefficients (D) were determined by the ultramicroelectrode CV technique of Baranski and the Cottrell equation.[27] The heterogeneous rate constants k_s were calculated according to the Klingler-Kochi method as the potential difference for the anodic and cathodic peak currents for the second peak was more than 460 mV.[28] k_s values under these circumstances depend on the scan rate, diffusion coefficient, and oxidation and reduction peak potential values. All the values are tabulated in Table 4.

The oxidation of formazan and their nickel(II) complexes was found to be quasi-reversible due to the fact that ΔE_p is larger than 59/n (mV), which increased with the scan rate, and the shift of the anodic peak potential E_{ox} towards positive values with increasing scan rate. Change in the k_s values was in the order of

Table 4. Some of the parameters calculated for formazans (**1a-4a**) and nickel(II) complexes (**1b-4b**).

No	Abbreviation	C* (ml)	i_{ss}/A	Cottrell Slope (S)	n	n net	D (cm^2/s)
1a	TPF (peak 1)	7.3	9.081×10^{-10}	1.599×10^{-5}	0.75	1	4.297×10^{-6}
1a	TPF (peak 2)	7.3	1.621×10^{-9}	2.109×10^{-5}	0.73	1	7.880×10^{-6}
2a	*o*-NNF	4.4	2.731×10^{-9}	3.076×10^{-5}	1.58	2	1.051×10^{-5}
3a	*m*-NNF	6.2	9.310×10^{-9}	2.361×10^{-7}	1.81	2	1.946×10^{-5}
4a	*p*-NNF	7.3	4.751×10^{-9}	1.758×10^{-7}	1.67	2	8.430×10^{-6}
1b	Ni-TPF	7.8	4.417×10^{-10}	1.249×10^{-5}	0.88	1	1.667×10^{-6}
2b	Ni-*o*-NNF	8.7	7.860×10^{-9}	1.687×10^{-7}	0.78	1	2.341×10^{-5}
3b	Ni-*m*-NNF	6.3	9.282×10^{-9}	2.504×10^{-7}	2.01	2	1.908×10^{-5}
4b	Ni-*p*-NNF	7.7	3.781×10^{-10}	5.200×10^{-8}	1.55	2	6.360×10^{-7}

m-> *o*-> *p*-substitutions for $-NO_2$ substituted formazans and in the order of *o*-> *m*-> *p*-substitutions for nickel(II) complexes (Table 2). The k_s value of **3a** is larger than that of the other formazans and **2b** is larger than that of the other complexes. The resonance effect is smaller when the NO_2 group is at the *m*-position. E_{ox1} value is inversely proportional with the k_s value. Therefore anodic peak potential E_{ox1} shifts towards anodic values with the increase in standard heterogeneous rate constant k_s.

The calculation of the number of electrons transferred

The number of electrons transferred was obtained with the use of the chronoamperometric Cottrell equation.[27]

$$i_t = \frac{nFACD^{1/2}}{\pi^{1/2}t^{1/2}} \tag{1}$$

and ultramicrodisc electrode (UME) steady state current (I_{ss}) (Eq. 2).[28]

$$i_{ss} = 4rnFCD \tag{2}$$

The real surface area of the Pt electrode was found to be 2.58 cm^2 with the use of ferrocene. If i_t values are plotted against $t^{-1/2}$ the resulting slope (Eq. 3) will give the n value

$$Slope = \frac{1}{2}\left(\frac{nFCi_{ss}}{\pi r}\right)^{1/2} A \tag{3}$$

As seen from Table 4 and Figure 4a, there are 2 step 1 each electron transfer waves for **1a**, suggesting that the compound first gives a formazan radical (TPF), followed by the formation of a tetrazolium cation (TPT^+). **1a** is oxidized in 2 step each-electron transfer process to the corresponding tetrazolium cation (TPT^+). The possible mechanism of the oxidation of **1a** is shown in Scheme 3.

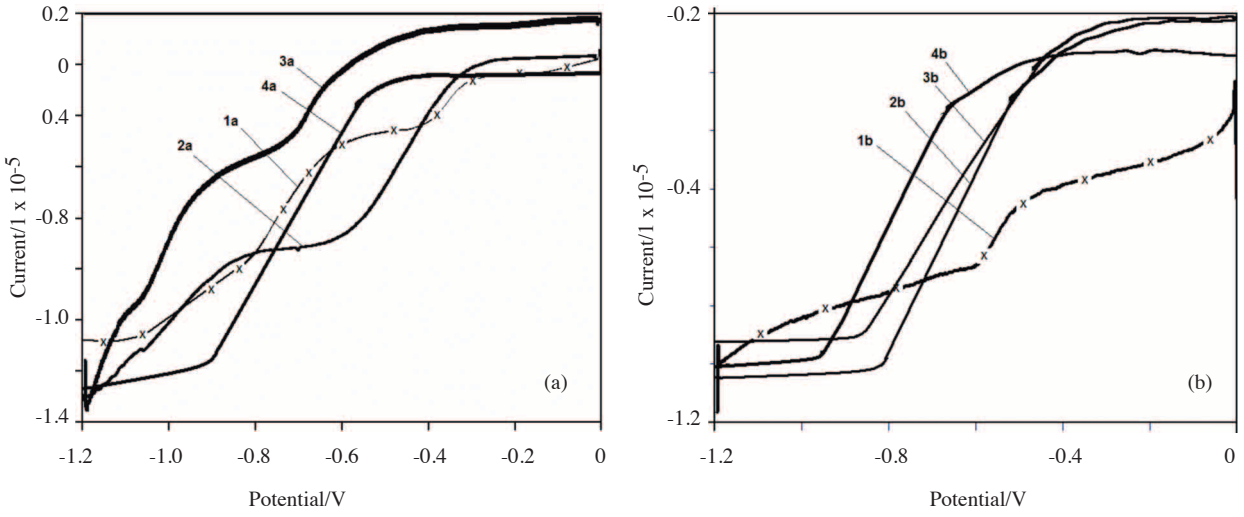

Figure 4. UME curves of (a)**: 1a-4a,** (b): **1b-4b** (DMSO solutions of 1.0×10^{-4} M in the presence of 0.1 M $TBA^+BF_4^-$ at 10 μm-platinum ultramicro electrode. Potential scan rate: 10 mV s^{-1}).

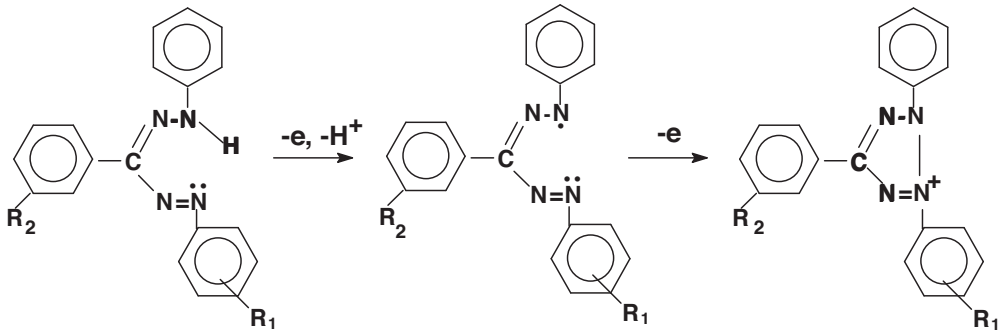

Scheme 3. Possible oxidation mechanism of **1a** and **3a.**

The number of electrons transferred was found to be 2 for **1a-4a** by the use of UME based cyclic voltammogramic and chronoamperometric data (Table 4). These results are in agreement with the literature.[22,25]

As seen from Figure 4a, there are 2 one-electron transfer waves for **3a**. In UME **3a** gave a clear S-shaped steady state current (I_{ss}). The number of electrons transferred was found to be 2 for **3a** using UME based cyclic voltammograms and chronoamperometric curves (Table 4). This is in accordance with CV results (Figure 2). **3a** are oxidized in 2 quasi-reversible 2-electron processes to the corresponding tetrazolium cation. The mechanism of the oxidation of **3a** is shown in Scheme 3a. These results are in agreement with the literature.[22,25]

As seen from Table 4 and Figure 4a, there are 1-step 2-electron transfer waves for the case of **2a** and **4a,** which is oxidized with a single quasi-reversible 2-electron process to its corresponding tetrazolium cation. The mechanism of the oxidation of **2a** and **4a** is shown in Scheme 4. These results are in agreement with the literature.[22,25]

As seen from Figure 4b and Table 4, there is a 1-electron transfer wave for **1b**. There are Ni^{2+} and TPF^- anions (**X**) present in the solution (Scheme 5). TPF^- anion gives a single 1-electron transfer giving a formazan radical (TPF). These radicals give a disproportionation reaction resulting in a formazan (TPF)

and tetrazolium cation (TPT^+) or a dimerization reaction resulting in a diformazan. The mechanism of the oxidation of **1b** is shown in Scheme 5. These results are in agreement with the literature.[21,24,26]

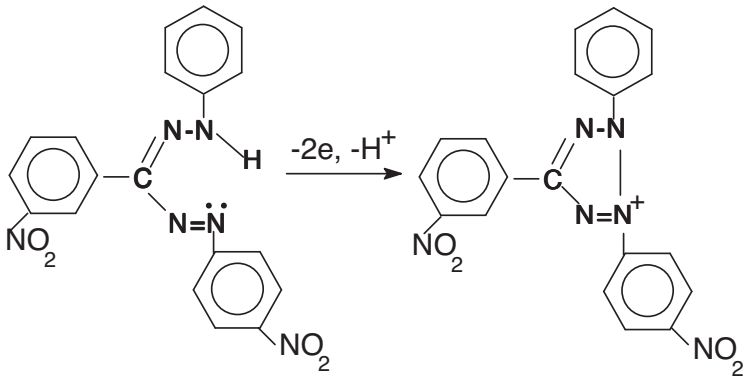

Scheme 4. Possible oxidation mechanism of **2a** and **4a**.

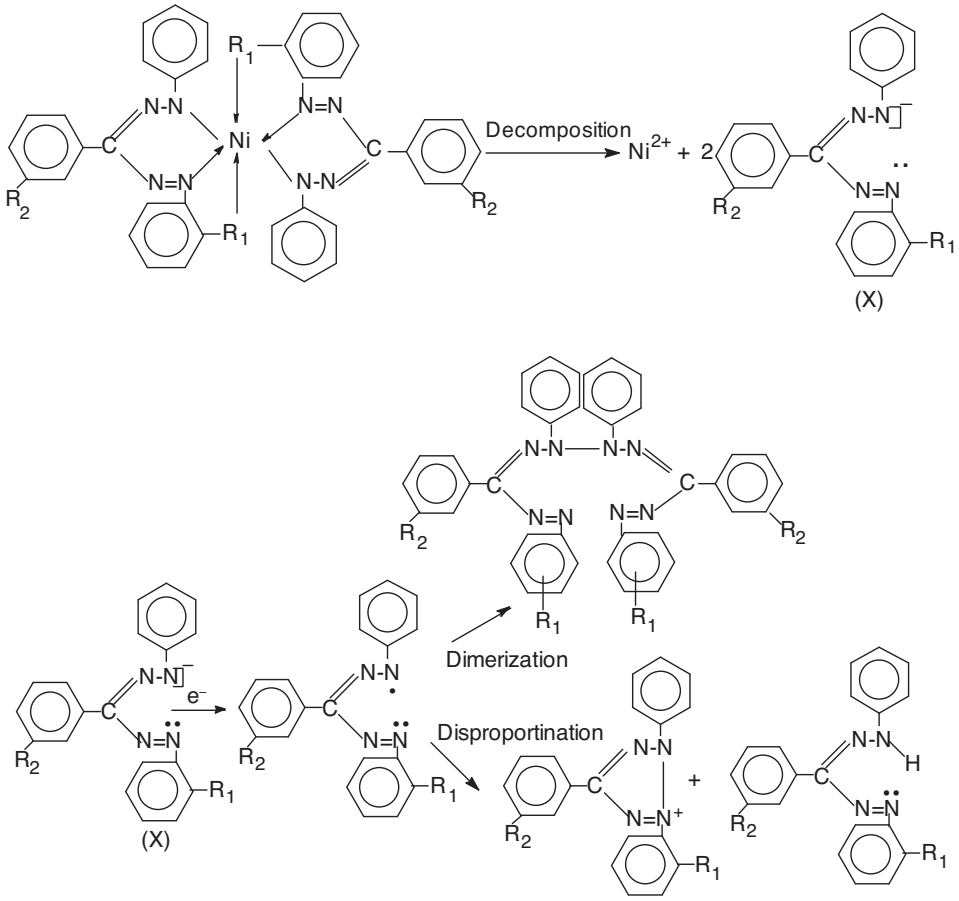

Scheme 5. Possible oxidation mechanism of **1b**, **2b.**

The appearance of 1 distinctive peak for **2b** also suggests that the compound gives 1 electron transfer. This was clearly the case since the number of electron transferred was found to be 1 for **2b** according to UME and

chronoamperometric data. This is in accordance with CV results. **2b** is fragmented and Ni^{2+} and substituted formazan radicals are formed in solution (**Scheme 5**). These radicals undergo a disproportionation reaction giving a substituted formazan and tetrazolium cation or a dimerization reaction resulting in a diformazan. The mechanism of the oxidation of **2b** is shown in Scheme 5. These results are in agreement with the literature.[21,24,26]

As seen from Figure 4b there are 2-electron transfer waves and the number of electrons transferred was found to be 2 for **3b** and **4b** from UME and chronoamperometric data (Table 4). This complies well with the CV results (Figure 3). The appearance of 2 distinctive peaks for **3b** and **4b** suggests that these compounds give 2-electron transfer. **3b** and **4b** are fragmented giving Ni^{2+} and substituted formazan radicals in the solution. **3b** and **4b** form substituted formazan radical giving corresponding tetrazolium cation by losing 2 electrons. The mechanism of the oxidation of **3b** and **4b** is similar to Scheme 4. These results are in agreement with the literature.[22,24,26]

The relation between the λ_{max} with E_{ox1} and E_{red1} values

There was a correlation between absorption λ_{max} values of NO_2 substituted formazans and their Ni complexes (**2a-4a, 2b-4b**) with their oxidation and reduction peak potentials (Figures 5 and 6).

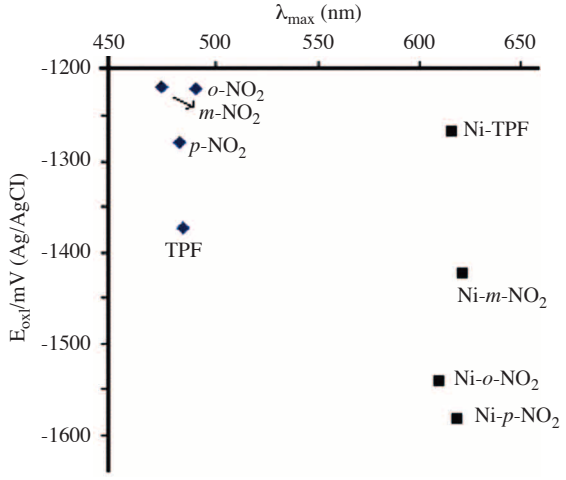

Figure 5. The correlation between the λ_{max} values and the E_{ox1} /mV (Ag/AgCl) values of **1a-4a** and **1b-4b**.

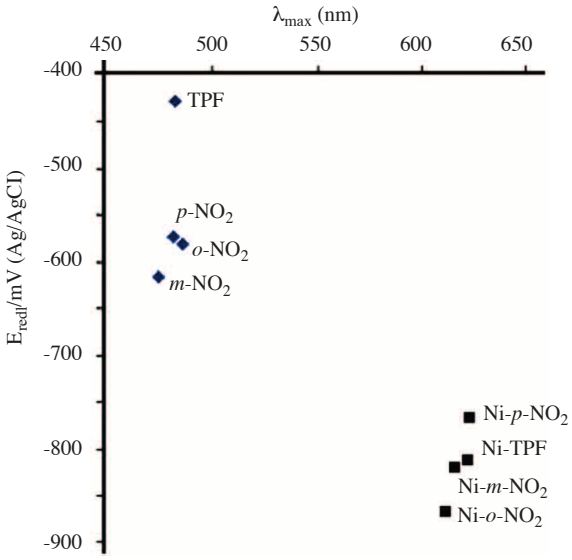

Figure 6. The correlation between the λ_{max} values and the E_{red1} /mV (Ag/AgCl) values of **1a-4a** and **1b-4b**.

Conclusions

In this study the peak potentials (E_{ox} , E_{red}), diffusion coefficients (D), number of electrons transferred (n), and heterogeneous rate constants (k_s) of formazans and their nickel(II) complexes were determined and a possible oxidation mechanism was proposed. Moreover, the spectral and the electrochemical behaviors of the formazans

and their Ni complexes were compared.

Electrochemical reaction mechanisms are dependent upon the type and position of the substituent in the structure. Consequently, both the electrochemical and spectral properties are dependent upon the type and position of the substituent in the structure. These results were expected, because, consequently, both absorption and electron features depend on the electron density of molecular systems.

Acknowledgements

We are very grateful to the Gazi University Research Fund for providing financial support for this project (No. 04/2004-13).

References

1. Von Pechmann, H. *Ber. Detsch. Chem.* Ges. **1894**, *27*, 1679.
2. Hunter, L.; Roberts, C. B. *J. Chem. Soc.* **1941**, *9*, 820-823.
3. Lewis, J. W.; Sandorfy, C. *Can. J. Chem.* **1983**, *61*, 809-816.
4. Katritzky, A. R.; Belyakov, S. A.; Cheng, D.; Durst, H. D. *Synthesis* **1995**, *5*, 577-581.
5. Arnold, G.; Schiele, C. *Spectrochim. Acta* **1969**, *25A*, 685-696.
6. Yüksel U. Post Doctoral thesis. Aegean Univ. (in Turkish).
7. Tezcan, H.; Uyar, T.; Tezcan, R. *Turkish J.Spect. Aegean Univ.* **1989,** *X(1)*, 82-90.
8. Tezcan, H.; Uzluk, E. *Dyes Pigments* **2007**, *75(3)*, 633-640.
9. Czajkowski, W.; Stolarski, R.; Szymczyk, M.; Wrzeszcz, G. *Dyes Pigments* **2000**, *47*, 143-149.
10. Gok, Y.; Tufekci, M.; Ozcan, E. *Synth. React. Inorg. Met.-Org. Chem.* **1993**, *23*, 861-873.
11. Tezcan, H.; Uzluk, E. *Dyes Pigments* **2008**, *76*, 733-840.
12. Sigeikin, G. I.; Lipunova, G. N.; Pervova, I. G. *Russ. Chem. Rev.* **2006**, *75*, 885-900.
13. Brown, D. A.; Bögge, H.; Lipunova, G.N.; Müller, A.; Plass, W.; Walsh. K. G. *Inorg. Chim. Acta.* **1998**, *280*, 30-38.
14. Issa, Y. M.; Rizk, M. S.; Tayor, W. S.; Soliman, M. H. *J. Ind. Chem. Soc.* **1993**, *70,* 5-7.
15. Uchiumi, A.; Takatsu, A.; Tanaka, H. *Anal. Sci.* **1991**, *7,* 459-62.
16. Kawamura, Y.; Yamauchi, J.; Ohya-Nishiguchi, H. *Bull. Chem. Soc. Jpn.* **1993**, *66*, 3593-3599.
17. Schiele, V. C. *Ber.* **1964**, 30, 308-318.
18. Mattson, A. M.; Jensen, C. O.; Dutcher, R. A. *Sci.* **1947**, *5*, 294-295.
19. Wan, H.; Williams, R.; Doherty, P.; Williams, D. F. *J.Mater. Sci.: Mater. in Med.* **1994**, *5*, 154-159.
20. Umemoto, K. *Bull. Chem. Soc. Jpn.* **1989**, *62*, 3783-3789.
21. Abou Elenien, G. M. *J. Electroanal. Chem.* **1994**, *375*, 301-305.
22. Oritani, T.; Fukuhara, N.; Okajima, T.; Kitamura, F.; Ohsaka, T. *Inorg. Chim. Acta* **2004**, *357*, 436-442.

23. Gökce, G.; Durmus, Z.; Tezcan, H.; Yılmaz, H.; Kılıc, E. *Anal. Sci.* **2005**, *21*, 1-4.

24. Tezcan, H.; Uzluk, E.; Aksu, M. L. *Electrochim. Acta A.* **2008**, *53*, 5597-5609.

25. Tezcan, H.; Uzluk, E.; Aksu, M. L. *J. Electroanal. Chem.* **2008**, *619-620*, 105-516.

26. Tezcan, H.; Uzluk, E.; Aksu, M. L. *Spectrochim. Acta. B.* **2008**, *70*, 973-982

27. Baranski, A. S.; Fawcett, W. R.; Gilbert, C. M. *Anal. Chem.* **1985**, *57*, 166-170.

28. Klingler, R. J.; Kochi, J. K. *J. Phys. Chem.* **1981**, *85*, 1731.

29. Williams, D. H.; Fleming, I. *Spectr. Meth. in Org. Chem.* McGraw-Hill Publishing Company Limited, London, 1966.

30. Bard, A. J.; Faulkner, L. R.; *Electrochem. Meth.:* Fundementals and Applications, 2^{nd} ed. John Wiley & Sons, Newyork (2001).